Polyacetylene oligomers: π-electron fluctuations, vibrational intensities, and soliton confinement

Anna Painelli, Luca Del Freo, and Alberto Girlando
Dipartimento di Chimica Generale ed Inorganica, Chimica Analitica e Chimica Fisica, Università di Parma, I-43100 Parma, Italy

Zoltan G. Soos
Department of Chemistry, Princeton University, Princeton, New Jersey 08544
(Received 12 April 1999)

We present a simple, internally consistent model for calculating ground-state properties of polyacetylene (PA) oligomers. The model describes π electrons according to Hückel theory and accounts for electron-phonon coupling with an exponential dependence of hopping integrals on the bond length. Careful tuning of model parameters against the geometry and Raman frequencies of pristine PA allows the calculation of vibrational frequencies and nonresonant Raman intensities of oligomers, as well as infrared active vibrational spectra of solitons on short chains. The available experimental data are well reproduced by the proposed model. Both infrared and nonresonant Raman intensities are found to scale superlinearly with the chain length. By relating this behavior to the scaling of the optical gap, we gain insight on the coherence length of π-electron motion in PA. [S0163-1829(99)04635-4]

I. INTRODUCTION

Conjugated polymers are an interesting playground for testing the robustness of theoretical models. Although conjugated polymers are characterized by similar C-C bonds, they show a large variety of physical properties. The challenge for theorists is to devise interpretative models that account for different physical properties in terms of a consistent unifying scheme. Quantum chemistry models offer very accurate descriptions of most molecular properties, but *ab initio* approaches are too detailed to extract a simple physical picture for conjugation. Transferring *ab initio* tools to polymers is not easy either, since accurate basis sets are restricted to rather short oligomers. On the other hand, the peculiar and interesting properties of conjugated polymers are governed by π electrons. Semiempirical models are appealing in view of their simplicity and are widely used for ground and excited states of conjugated polymers.

In recent years much data have been collected on low-lying excitations of conjugated polymers, based essentially on linear and nonlinear optical experiments.[1] These data put into evidence the importance of Coulomb interactions, especially in excited states, and have been analyzed using the Pariser-Parr-Pople model.[2] The problem of modeling π electrons is considerably simpler if one concentrates only on ground-state (GS) properties. Hückel theory is generally adequate, without explicit e-e interactions, provided that parameters are carefully extracted from experiment. But electron-phonon coupling is crucial for modeling GS properties of conjugated polymers. The Su-Schrieffer-Heeger (SSH) model[3] contains a linear dependence of the hopping integral $t(r)$ on the bond distance. An exponential $t(r)$ is certainly preferable, as recognized in early studies of conjugated molecules.[4]

Ground-state properties include the equilibrium bond lengths of polymers, oligomers, and of their defect states, linear and nonlinear polarizabilities at low frequency, and vibrational properties such as frequencies, infrared (IR), and nonresonant Raman intensities. A Hückel approach to π electrons with electron-phonon (e-ph) coupling is expected to be adequate for these properties when augmented with a model for the elastic energy due to σ electrons. In our previous studies of PA vibrational spectra, we adopted a strictly empirical approach to the elastic energy. We distinguished two contributions to the vibrational force field:[5] a reference contribution for the sum of the force fields due to σ electrons and the π-electron GS, and a contribution from π-electron fluctuations. Detailed Raman analysis of pristine PA and of its isotopically substituted analogs allowed us to obtain the reference force field for pristine PA.[5,6] Moreover, our analysis unambiguously led to the exponential $t(r)$.[7] It has been extended to Raman spectra of *cis*-PA,[7] of PA oligomers,[8] and, phenomenologically, to vibrational spectra of soliton defects in *trans*-PA.[5]

In this paper we present a more general model for GS properties of PA and its oligomers, using a Hückel model with an exponential $t(r)$. This choice immediately implies the functional form for effective σ and reference force fields.[4] We extract the few model parameters from PA data. We have therefore an internally consistent model for π and σ electrons in PA chains. The model allows the calculation of the backbone geometry of oligomers as well as solitons on chains of variable lengths, and of vibrational spectra of both oligomers and solitons. Our results on vibrational frequencies, IR, and nonresonant Raman intensities agree well with available experimental data, proving the reliability of the proposed approach. The nonresonant Raman intensities of PA oligomers or the IR intensities of solitons show a distinctly superlinear dependence on the chain length, proving the intimate relation between vibrational properties and π-electron fluctuations. The Raman and IR intensities scale with different powers of the optical gap offering information on the coherence length of π-electron motion in PA. The simple model reliably describes the physics underlying the peculiar vibrational properties of conjugated polymers, and opens the way to understanding the subtle interplay of elec-

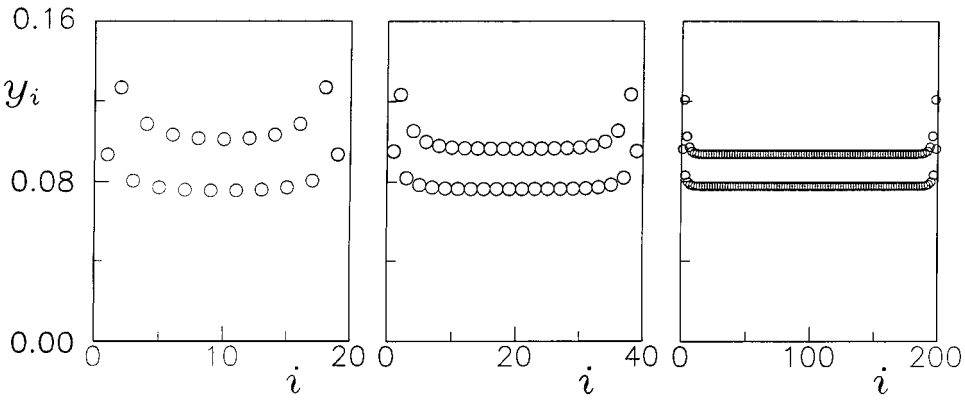

FIG. 1. The geometry of PA oligomers with $N=20$, 40, 200; y_i is measured in Å.

tronic and vibrational degrees of freedom in determing the macroscopic properties of conjugated materials.

II. GEOMETRY AND VIBRATIONS: FIXING THE PARAMETERS AGAINST PRISTINE PA

The physics of conjugated polymers is dominated by the large coherence length of π electrons as compared to the local nature of σ electrons. The simplest general model for π electrons is the Hückel Hamiltonian,

$$H_e=-\sum_{i,\sigma} t_i(c^{\dagger}_{i+1,\sigma}c_{i,\sigma}+\text{H.c.})=-2\sum_i t_i\hat{b}_i, \qquad (1)$$

where $c_{i,\sigma}$ is the annihilation operator for an electron with spin σ on the ith site, t_i is the resonance integral for the ith bond, and $\hat{b}_i$ is the bond-order operator. In pristine PA, the ground state is dimerized with alternating transfer integrals t_s and t_d for single and double bonds, respectively. The standard value for the mean t, $t^0=2.5$ eV, and the optical gap of PA fixes the alternation parameter $\delta=(t_d-t_s)/(t_d+t_s)=0.18$.

The SSH model[3] has linear $t(r)$, $t_i=t^0-\alpha r_i$, with r_i measuring the deviation of the ith bond length from a hypothetical uniform chain. But exponential $t(r)$ has long been known to be more realistic.[4] Whereas the essential physics of the e-ph coupling in conducting polymers follows from the linear e-ph coupling, accurate analysis of vibrational spectra requires more refined models. The Raman spectra of pristine PA point to different α values for single and double bonds:[7] $\alpha_d=6.4$ eV/Å and $\alpha_s=4.1$ eV/Å. This result strongly supports an exponential dependence:

$$t_i=t^0\exp(-\gamma r_i). \qquad (2)$$

In fact, the ratio $\alpha_s/\alpha_d=0.64$ agrees within 10% with the ratio of the corresponding t's: $t_s/t_d=0.69$. For $t^0=2.5$ eV, the empirical α value fix $\gamma=2.1$ Å^{-1}.

σ electrons are not explicitly included in the Hückel model, but originate a local vibrational potential. The total energy of the chain is then the sum of a π-electron contribution [as described by Eq. (1)] plus the vibrational potential of the σ electrons. Consistently with the Hückel approximation, we describe the vibrations of a linear PA chain. The generalization of the results to account for the actual zigzag structure of PA is fairly natural and will be discussed in due course. Following Longuet-Higgins and Salem's classic paper,[9] the vibrations of the σ skeleton are modeled as a sum of independent bond oscillations:

$$V^{\sigma}=\sum_i f(r_i). \qquad (3)$$

The equilibrium condition is found by minimizing, for each bond, the total $(\sigma+\pi)$ energy:

$$f'(r_i)-2b_it'_i=0, \qquad (4)$$

where the prime indicates the derivative with respect to r_i evaluated at the equilibrium and b_i is the ground-state expectation value of the Coulson bond order. By further differentiating the above equation and using the exponential $t(r)$ dependence, we get

$$f''(r_i)=K_i^{\sigma}=-2b'_it_i\gamma+2\gamma^2t_ib_i. \qquad (5)$$

b_i can be easily calculated for any given H_{el} in Eq. (1), whereas b'_i is more difficult. Following Coulson and Longuet-Higgins,[10] we set b'_i to a constant: $-2b'_i=A$, with A chosen to reproduce the bond-length alternation of pristine PA in our case.

By definition $f''(r_i)$ is the harmonic force constant relevant to the stretching coordinates of the ith bond (K_i^{σ}), so that, by describing the σ potential in the (locally) harmonic approximation, the total $\sigma+\pi$ energy is written as follows:

$$E_G^{\sigma+\pi}=\frac{1}{2}\sum_i (K_i^{\sigma}R_i^2-2t_ib_i)=\frac{1}{2}\sum_i \{(A\gamma t_i+2\gamma^2t_ib_i) \times[r_i-(r_i)_{\text{eq}}]^2-2t_ib_i\}, \qquad (6)$$

where R_i, measuring the deviation of the ith bond from the equilibrium length, is the standard stretching coordinate.[11] Minimization of the energy in Eq. (6) leads to an unphysical collapse of the structure.[12] Different constraints have been proposed to avoid collapse.[12–15] We choose to fix the mean $t=t^0$ during the minimization steps, so that the energy scale is kept constant. The equilibrium geometry is then found by self-consistently minimizing the total energy. Starting with trial bond lengths, we solve the electronic Hamiltonian and calculate bond orders. They are inserted into Eq. (6) and are kept constant during the energy minimization. The new equilibrium position is then used to restart the procedure. The process is repeated until the relative variation in $(r_i)_{\text{eq}}$ is less than 0.1%.

In Fig. 1 we report the absolute value of the deviations of

the bond lengths from the uniform lattice, $y_i=(-1)^i(r_i)_{\rm eq}$, as obtained for PA oligomers with $N=20$, 40, and 200 sites, and $A=3.20$ Å^{-1}. Finite-size effects are evident at the chain ends, but a region of uniform dimerization, independent of the chain length, clearly develops in the middle. This region describes bulk PA, and we fix the A value as to regain $\delta=0.18$ there. The SSH model[3] has constant y_i in pristine PA: single bonds lengthen with respect to the regular chain by the same amount as the double bonds shrink. We calculate instead different y_i for single and double bonds, with double bonds shortening by $y_{2n+1}\sim 0.077$ Å with respect to the regular chain, and the single bonds lengthening by $y_{2n}\sim 0.094$ Å. This difference originates from the nonlinearity introduced by an exponential $t(r)$, with larger distortions at single than at double bonds. The mean displacement of each site is calculated as $(y_{2n+1}+y_{2n})/4\sim 0.043$ Å, in agreement with structural data.[16]

Vibrational spectra of conjugated polymers are conveniently analyzed using the Herzberg-Teller formalism, which is a perturbative expansion of the GS energy and wavefunction on vibrational coordinates.[17] In this approach the π contribution to the vibrational force constants (K_i^π) is naturally separated in two terms:

$$K_i^\pi=\langle G|\frac{\partial^2 H_e}{\partial R_i^2}|G\rangle-2\sum_F \frac{\langle G|\frac{\partial H_e}{\partial R_i}|F\rangle\langle F|\frac{\partial H_e}{\partial R_i}|G\rangle}{E_F^\pi-E_G^\pi}, \quad (7)$$

where $|G\rangle$ and $|F\rangle$ are the ground and the excited states of H_e, and E_G^π and E_F^π are the corresponding energies. The first term above only involves the ground-state π-electron distribution and adds to K_i^σ to define a reference force constant, K_i^0. The second term accounts for π-electron fluctuations and is responsible for the peculiar vibrational properties of conjugated polymers.[5]

The reference force field F^0 can be extracted from vibrational data using standard techniques.[11] For pristine PA, F^0 has already been obtained, based on the butadiene force field, and has been successfully applied to Raman frequencies.[5,6] The reference force field for the linear PA that we consider in this paper minimally requires different force constants for stretching single and double C-C bonds, $K_s^0=36.25$ eV/Å^2 and $K_d^0=50.625$ eV/Å^2, respectively, and an interaction between adjacent stretches, $K_{12}=1.67$ eV/Å^2.[6] In either finite chains or in the presence of a topological defect, several kinds of C-C bonds are found in general, rather than just partial single and double bonds. One therefore needs a recipe to associate a reference force constant to each C-C bond. The π-electron contribution to F^0 [the first term in the right-hand side of Eq. (7)] is calculated from the Hamiltonian in Eq. (1):

$$\langle G|\frac{\partial^2 H_e}{\partial R_i^2}|G\rangle=-2t_i''b_i. \quad (8)$$

This term exactly cancels the second term in K_i^σ in Eq. (5), so that the reference force constant for the bond stretch turns out to be proportional to the corresponding hopping integral:

$$K_i^0=A^*\gamma t_i. \quad (9)$$

In principle, the A^* parameter in the above equation should correspond to the A parameter adopted in the geometry optimization. This choice, however, leads to unphysically small force constants. Therefore, we fix A^* against the reference force constants for C-C stretches, as previously extracted from the analysis of the Raman spectra of pristine PA.[6] In particular, by comparing the experimental value of the mean force constant, $(K_d^0+K_s^0)/2\sim 43.44$ eV/Å^2, with the mean t value, we get $A^*=8.30$ Å^{-1}. The A^* value turns out more than twice the A value adopted for the geometry optimization. It is quite common for semiempirical models that different parameter values have to be chosen in order to fit different properties. In early approaches to π-conjugated systems,[4] bond lengths and force constants have been modeled with the same $A=-2b'$, but this choice required an effective t^0 value less than half the spectroscopic t.[4] In our approach instead we fix t^0 to the spectroscopic value (~ 2.5 eV), and adjust independently A and A^* as to reproduce PA geometry and force constants: the discrepancy between A and A^* parallels the well known discrepancy between the spectroscopic t and the t evaluated from vibrational data.[4]

III. PA OLIGOMERS: THE ROLE OF π-ELECTRON FLUCTUATIONS

For pristine PA chains the bond lengths calculated according to the preceding section fix the reference force field, $\mathbf{F^0}$. The geometry also defines the **G** matrix (the inverse of the kinetic energy matrix). The reference frequencies and normal modes can be obtained by diagonalizing the $\mathbf{GF^0}$ matrix. By Fourier-analyzing the reference normal modes into the wave-vector space, we assign each normal mode an effective wave-vector (q), corresponding to its Fourier component with the largest amplitude.[2,18] Of course, by increasing the chain length, the normal modes become essentially pure q states. In order to avoid ambiguities with the q labeling, we adopt the extended Brillouin-zone representation, as relevant to an undimerized PA chain.

The reference vibrational problem describes a hypothetical chain with π electrons frozen in their ground-state configuration. The spectroscopic anomalies of conjugated polymers and oligomers are instead associated with the coupling of phonons to the large π-electron fluctuations. The total force field is written on the basis of the reference normal coordinates (Q_q^0) as the sum of the reference force field, which corresponds to the diagonal matrix of the squared reference frequencies (ω_q^0), and the contribution from π-electron fluctuations, as follows:

$$\Phi_{q,q'}=\omega_q^0\omega_{q'}^0\delta_{q,q'}+\Delta\Phi_{q,q'}=\omega_q^0\omega_{q'}^0\delta_{q,q'}+\left(\frac{\partial^2 E_G^\pi}{\partial Q_q^0\partial Q_{q'}^0}\right)_{\rm lin}, \quad (10)$$

where the ''lin'' index in the derivative implies that it is calculated by linearizing $t(r)$ around the equilibrium position. This linearization, which is irrelevant in the SSH model, is needed to avoid double-counting second derivatives of $t(r)$ that are already contained in the reference force field.

In the infinite chain, due to translational symmetry, only the $q=\pi$ mode is of interest for optical spectroscopy. This mode, the extended conjugation coordinate (ECC) by Zerbi,[19] describes the out-of-phase stretching of adjacent C-C bonds. It is a totally symmetric, Raman-active mode. Since in long chains the wave vector is a good quantum number, mixed derivatives in Eq. (10) involving Q_π^0 vanish, so that the squared vibrational frequency at $q=\pi$ is simply given by the diagonal element of the above force field:

$$\omega_\pi^2=(\omega_\pi^0)^2+\Delta\Phi_{\pi\pi}. \tag{11}$$

For short chains this equality is not granted *a priori*. Therefore, we go back to internal coordinates (R_i) and, following Coulson and Longuet-Higgins,[10] we directly calculate the contribution of π-electron fluctuations to the vibrational force field as

$$\Delta F_{ij}=-\frac{8}{N}\frac{\partial t_i}{\partial R_i}\frac{\partial t_j}{\partial R_j}\sum_F \frac{\langle G|b_i|F\rangle\langle F|b_j|G\rangle}{E_F^\pi-E_G^\pi}. \tag{12}$$

The above matrix elements are easily calculated in terms of the energies and coefficients of the Hückel molecular orbitals MO.[4] The electronic elements are the π-electron bond-bond polarizability. The total force field in internal coordinates is simply the sum of the reference force field plus the above correction: $\mathbf{F}=\mathbf{F^0}+\mathbf{\Delta F}$. Diagonalization of the **GF** matrix yields an independent estimate of vibrational frequencies. By inserting this estimate of ω_π in Eq. (11), we find that the equality is satisfied within 1% even for butadiene ($N=4$). Therefore, although there is no symmetry requirement for short chains, the Q_π^0 mode is not appreciably mixed by e-ph coupling to vibrational modes with different wave vectors.

Due to the actual zigzag backbone of pristine PA, C-C-C and C-C-H bendings mix with the ECC mode so that three bands appear in Raman spectra.[5,7] The same three modes are easily recognized in oligomers:[20,21] the highest and lowest frequency bands, ν_1 and ν_3, respectively, observed at $\sim$1469 and 1079 cm^{-1} in PA, shift to higher frequencies in oligomers, up to $\sim$1623 and 1188 cm^{-1} for $N=6$. The weak band at $\sim$1290 cm^{-1} (ν_2) is practically unaffected by chain length. In our previous phenomenological analysis, we showed that the Raman frequencies of PA oligomers are well reproduced by adopting the same reference force field as for pristine PA, and imposing that the coupling of the ECC mode to π electrons is scaled by an amount χ, with respect to that relevant for pristine PA ($\chi=1$).[6,2] Since the reference force field is based on butadiene, it already accounts for (small) π-electron fluctuations in this short polyene.[22] Therefore, the phenomenological χ values, as extracted from the Raman frequencies of PA oligomers, can be compared with the theoretical relative χ, defined by

$$\chi(N)=\frac{(\Delta\Phi_{\pi\pi})_N-(\Delta\Phi_{\pi\pi})_{N=4}}{(\Delta\Phi_{\pi\pi})_{N=300}-(\Delta\Phi_{\pi\pi})_{N=4}}, \tag{13}$$

where the $N=300$ chain mimics pristine PA. The good quantitative agreement between the calculated and experimental χ, as reported in Fig. 2, upper panel, demonstrates the reliability of the proposed approach to calculate vibrational properties of PA oligomers. We underline that similar χ values have been reported in Refs. 2 and 22 for oligomers up to

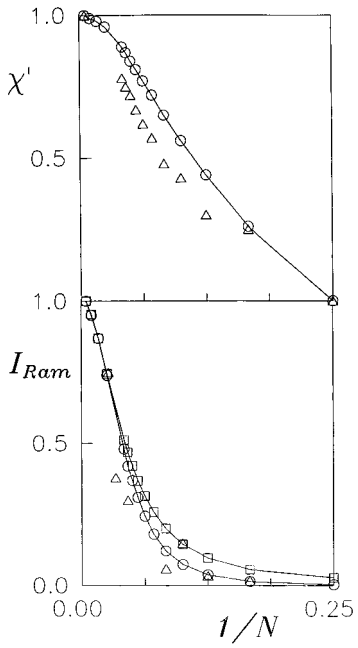

FIG. 2. PA oligomers. Upper panel: the relative χ vs $1/N$; circles and triangles refer to numerical results and to experimental data, respectively. Lower panel: the Raman intensity vs $1/N$; circles and triangles refer to numerical results and to experimental data, respectively; squares refer to the calculated $1/\Delta^4$, scaled to the value relevant to $N=200$. Lines are drawn to guide the eye.

14 sites in the Pariser-Parr-Pople model with an effective alternation $\delta=0.07$. As for electronic properties,[2] vibrational properties calculated in the Hückel and PPP approaches are comparable, provided that in both cases the effective alternation is fixed so as to reproduce the experimental optical gap.

We can now understand why the phenomenological approach to Raman spectra of PA oligomers works well. In fact, this approach implicitly relies on two assumptions: first of all, a single mode is strongly coupled to π electrons irrespective of the chain length, and second, the reference frequencies do not depend on N. We already proved that the first assumption is very well satisfied down to the shortest chain. On the other hand, the difference between the reference frequencies calculated for $N=4$ and $N=300$ is less than 10%. Such uncertainties are acceptable in interpretative models and are comparable to uncertainties in experimental evaluations of χ.

We turn next to the N dependence of the Raman intensity. It is known from experiments on several families of conjugated polymers that nonresonant Raman intensities increase superlinearly with the chain length.[23,24] The nonresonant Raman intensity can be calculated from the derivatives of the GS π-electron static first polarizability (α) on the vibrational coordinates. The static polarizability is the second derivative of the GS energy with respect to an applied electric field, so that its definition is formally similar to the π-electron contributions to the force field in Eq. (12):

$$\alpha=2\sum_F \frac{\langle G|\hat{\mu}|F\rangle\langle F|\hat{\mu}|G\rangle}{E_F^\pi-E_G^\pi}, \tag{14}$$

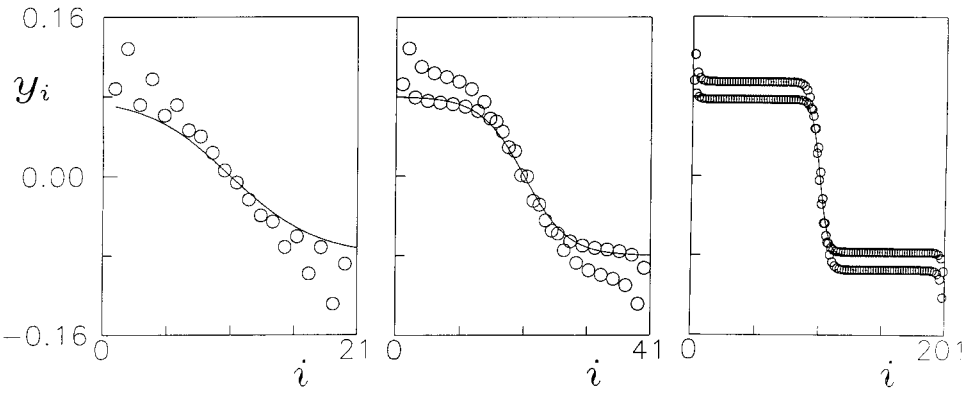

FIG. 3. The geometry of a soliton in PA chains with $N=21$, 41, 201. y_i is measured in Å.

where $\hat{\mu}$ is the dipole moment operator. For the infinite chain, only the $q=\pi$ mode has appreciable intensity, but the intensity of the same mode stays one order of magnitude larger than that of other modes even in short chains. In Fig. 2, lower panel, we report, as a function of the chain-length, the Raman intensity calculated as

$$I_{\mathrm{Ram}} \propto \frac{1}{N}\left(\frac{\partial \alpha}{\partial Q}\right)^2, \tag{15}$$

where we scale by the chain length in order to properly have an intensive property of the material. In Fig. 2, calculated intensities are compared with the available experimental results for PA oligomers.[23] In the absence of data on longer chains, we scale in such a way that the calculated and experimental intensities coincide for $N\sim 40$. The experimental data are affected by fairly large uncertainties, but compare favorably with the calculated intensities.

IV. SOLITONS IN FINITE CHAINS

The procedure in Sec. II for calculating the ground-state bond lengths can be directly applied to chains bearing a soliton defect. In fact, the soliton geometry describes the GS of a $2n+1$ chain, either the neutral radical or the singlet cation or anion. Due to the electron-hole symmetry of the Hückel Hamiltonian, the calculated bond lengths of neutral and charged solitons are equivalent. In Fig. 3, we report results for a soliton residing on chains with 201, 41, and 21 sites. For the sake of comparison, we also show the structure of a standard SSH soliton.[3] Since the soliton is a localized defect, extending approximately over 14 sites, there are no finite-size effects in long chains and the SSH soliton shape is essentially regained, as shown in Fig. 3 for $N=201$. The main deviation from the SSH shape is the larger distortions associated with single bonds with respect to double bonds, due to exponential $t(r)$. Of course this deviation, well evident in regions of large alternation, is reduced at the soliton center, where alternation reverses.

When the soliton is confined on short chains, end effects unavoidably alter its geometry, as clearly seen in Fig. 3 for $N=21$. Our empirical model for the soliton geometry is based on simple physical considerations and its only free parameter (A) is fixed against the known bond lengths of pristine PA. The mean bond length is not relevant for our model (the mean t is in fact fixed from the outset). We focus on the deviation of each bond from the length corresponding to the regular chain $[(r_i)_{\mathrm{eq}}]$. The calculated deviations are tiny in the middle of soliton defects.

Of course experimental data are not available, and results from *ab initio* calculations are too dependent on the choice of the basis set to allow for a sensible comparison.[25–27] We are not interested in bond lengths *per se*, rather we use them as the starting point for studying vibrational spectra. The validation of our approach to soliton geometries will be indirectly offered by the comparison with vibrational data.

The equilibrium geometry calculated for the soliton chain fixes the corresponding reference force field, $\mathbf{F^0}$, according to Eq. (9). Diagonalization of the $\mathbf{GF^0}$ matrix yields the reference frequencies and normal modes. Let us first discuss results for a long chain ($N=201$). Although translational symmetry is broken by the local defect, we still classify normal modes in terms of q, corresponding to the largest Fourier component. For long chains it is useful to distinguish between extended and local vibrations. The extension of each normal reference mode (Q_q^0) is approximately given by the inverse of the participation number, $p_q=\Sigma_j l_{qj}^4$, where l_{qj} are the coefficients of the vibrational eigenvectors, with j running on the sites. Similar to what happens for an SSH soliton,[18] a few local modes appear around a soliton defect, clustering in the regions $q\sim\pi/2$ and $q\sim\pi$. Once more a local mode at $q=\pi$ corresponds to the damped ECC (DECC). It describes the out-of-phase stretches of adjacent bonds, but with vanishing amplitude far from the soliton center.[18]

According to Eq. (10), we calculate for each reference normal mode the contribution of π-electron fluctuations to the force field. Quite predictably, the extended modes hardly change in the presence of a soliton, but behave like the modes of pristine chains. In Fig. 4, we report the diagonal elements of the $\mathbf{\Delta\Phi}$ matrix [see Eq. (11)], scaled to the $\Delta\Phi_{\pi\pi}$ value of the pristine chain. These data are similar to the π-electron susceptibilities that we reported for an SSH soliton.[18] The qualitative difference is that two local modes appear now at $q\sim\pi$, which are strongly coupled to π electron fluctuations. The strongest coupling is again to the DECC. This IR active coordinate describes the soliton translation and its coupling to π-electrons is about twice that of the extended mode at $q=\pi$. As we already found in the SSH model,[18] the IR intensity of DECC is about 4 orders of magnitude larger than that of other modes, so that DECC domi-

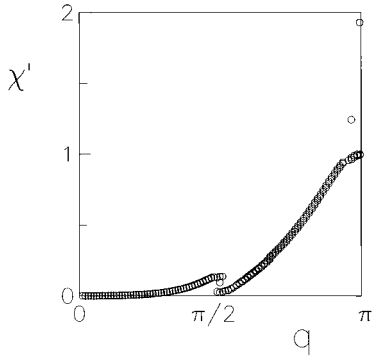

FIG. 4. The relative χ calculated for the reference normal modes of a soliton chain with $N=201$, as a function of the wave vector, q.

nates the IR spectra of doped or photoexcited PA samples.

The second localized mode, not found in the SSH soliton, is Raman active and its coupling to π electrons is ~ 1.2 times that of the $q=\pi$ extended mode. Its nonresonant Raman intensity, calculated from the first derivative of the GS π-electron susceptibility, is larger than the intensity of the extended mode at $q=\pi$. However, the soliton concentration in photoexcited or lightly doped ($<0.5\%$) (Ref. 16) samples is too small to detect this mode against bulk contributions. Heavily doped PA is of course beyond the scope of the present treatment.

Our results for charged solitons on long chains resemble those obtained with the linear e-ph coupling and SSH geometry.[18] Having a more realistic model and a method to obtain soliton bond lengths in finite chains, we can explore vibrational properties of solitons residing on short chains. In particular, we can model vibrational spectra of inhomogeneous PA samples.[28] By solving the reference vibrational problem for chains with N ranging from 5 to 301, we find a DECC mode for all chain lengths characterized by a large coupling to π electrons. It has large χ and IR intensity given by the the square of the derivative of the GS dipole moment, μ_G, with respect to the DECC,

$$I_{\mathrm{IR}} \propto \left(\frac{\partial \mu_G}{\partial Q} \right)^2 . \tag{16}$$

The upper panel of Fig. 5 shows the relative χ calculated for odd chains in accordance with Eq. (13). Once more we verified the consistency, within a few percent, of the calculated χ with the softening of the corresponding vibrational frequency as calculated by directly diagonalizing the **GF** matrix. There are insufficient photoexcitation data on PA chains of controlled length for direct comparison to χ. We notice, however, that the relative χ as reported in the figure for infinite chains agrees extremely well with the value extracted from the IRAV frequencies of photoexcited samples of pristine PA.[5] In Fig. 5, lower panel, we report the N dependence of the IR intensity, Eq. (16). The huge intensity is clearly related to the large π-electron fluctuations induced by the nuclear displacements along the DECC coordinate, and in this view we can easily understand its large increase with the chain length.

Polymers are intrinsically disordered materials and PA samples are characterized by a fairly wide distribution of

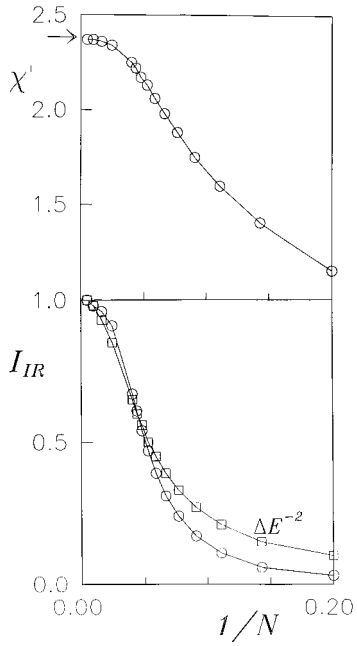

FIG. 5. Soliton chains. Upper panel: the calculated relative χ vs $1/N$; the arrow marks the experimental value for long chains. Lower panel: calculated IR intensity (circles) and $1/\Delta^2$ (squares). Lines are drawn to guide the eye.

chain lengths. The superlinear increase of the IR intensity of the DECC mode, associated with the early saturation of the $\chi(N)$ curve, leads to asymmetric IRAV band shapes even for a *symmetric* chain-length distribution. A soliton on chains ranging from $N=5$ to 201 is characterized by χ increasing from ~ 1 to ~ 2.3. From the empirical curves relating the vibrational frequencies to the effective χ,[5] we know that, for this variation of χ, the frequency of the highest vibrational mode (ν_1) is only slightly redshifted, whereas ν_3 experiences a huge redshift, from ~ 1100 cm^{-1} at $\chi \sim 1$ for $N=5$ to ~ 500 cm^{-1} at $\chi=2.3$ for $N=201$. Correspondingly, the weight of the DECC coordinate in the two modes varies. For short chains (low χ), the DECC contributes mainly to ν_1, whereas for longer chains (large χ) its weight moves to ν_3. The relative intensity of the two modes thus inverts between short and long chains. The mode at intermediate frequency stays practically unaffected by the e-ph coupling. In fact, at least for $(CH)_x$, the contribution of the DECC to this mode is very small, in agreement with its very small experimental intensity.[19]

We are now in the position to calculate IRAV spectra for any distribution of chain lengths. The vibrational problem for a soliton is fully defined by the complete reference force field as introduced in Ref. 5, and by the $\chi(N)$ reported in Fig. 5, upper panel. The reference force field in fact fixes the reference frequencies of the coupled modes, whereas the Raman frequencies of pristine PA fix the relative magnitude of the coupling constants.[5] The relative $\chi(N)$ then defines the vibrational problem for the soliton chain. Diagonalization gives, for each N, three IRAV frequencies $[\omega_\nu(N)]$ and the corresponding eigenvectors. By the way, the calculated frequencies are the same frequencies as reported as a function of χ in Fig. 1 of Ref. 5. The eigenvectors of the vibrational problem give information on the relative intensities of the

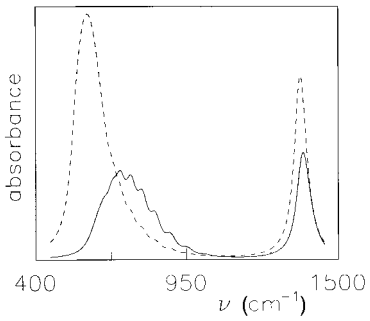

FIG. 6. Photoinduced IRAV spectrum calculated for a PA sample with a Gaussian distribution of chain lengths. Dashed lines: the Gaussian is centered at $N_0=25$, with $\Sigma=10$; continuous line: the Gaussian is centered at $N_0=15$, with $\Sigma=5$. In all calculations the intrinsic damping of Lorentzian curves [Eq. (17)] is set to $\Gamma=50$ cm^{-1}.

IRAV bands. Since the DECC is orders of magnitude more intense than other modes, we assign the three modes a relative intensity proportional to the weight of the DECC $[c_\nu^2(N)]$. We obtain the IR spectrum of a soliton residing on a chain of length N as the sum of three Lorentzians with fixed intrinsic damping (Γ), as follows:

$$\sigma_N(\omega)=\frac{I_{\mathrm{IR}}(N)}{2\pi}\sum_\nu \frac{c_\nu^2(N)\Gamma}{[\omega_\nu(N)-\omega]^2+(\Gamma/2)^2}. \qquad (17)$$

IRAV spectra of a disordered PA sample are then easily calculated by summing over the above $\sigma_N(\omega)$, weighted by a chosen distribution function, $P(N)$. In Fig. 6, we report two spectra calculated for different symmetric $P(N)$ distributions as described by a single gaussian centered at N_0 and with a standard deviation Σ: $P(N)=\exp[-(N-N_0)^2/2\Sigma^2]/\sqrt{2\pi}\Sigma$. As is apparent from the figure, asymmetric IRAV bands can be simulated in samples with symmetric chain-length distributions. The dashed line in Fig. 6 corresponds to the spectrum obtained for $N_0=25$ and $\Sigma=10$. This spectrum, with a broad, asymmetric band centered at $\sim$600 cm^{-1}, and a less intense and narrower band at $\sim$1360, simulates the IRAV bands as measured by photoexciting a well ordered sample like the stretched Durham PA.[28] As a continuous line we report the spectrum calculated for a distribution centered on much shorter chains, $N_0=15$, $\Sigma=5$. By shortening the chain length, the IRAV spectrum becomes considerably less intense. Moreover, the lowest band broadens, and its center moves upwards by more than 100 cm^{-1}. At the same time, the highest frequency band blueshifts to $\sim$1375, and acquires intensity at the expense of the lowest band. The behavior described in Fig. 6 for both ν_1 and ν_3 bands is quite consistent with experimental photoexcitation data collected on PA samples whose chain-length distribution is tuned by copolymerization.[28] While the simulated IRAV spectra in Fig. 6 do not prove symmetric chain-length distributions in actual PA samples, we underline that asymmetric distributions are neither needed nor demonstrated by asymmetric IRAV bands.

V. DISCUSSION

In this paper, based on simple physical considerations, we extend the Hückel model to account for the σ skeleton in an internally consistent picture. The few model parameters are fixed against experiment. We calculate the chain geometry of PA oligomers and soliton chains. The confinement of the soliton on short chains alters the soliton shape, whereas the standard SSH shape is regained on long chains. We also investigate the vibrational properties of PA oligomers and of solitons residing on chains of variable length.

The extension of the Hückel approach to the σ force field, as originally suggested by Coulson and Longuet-Higgins,[10] has already been applied to PA chains[29] as well as to conjugated polymers with nondegenerate GS.[30] These works have exponential t as in Eq. (2) and C-C bond lengths related to bond order as in Eq. (6), although with slightly different constraint to prevent chain collapse. The aims were to model backbone or conformational degrees of freedom in resonant Raman spectra and in electronic absorption and emission spectra. We model instead π-electron contributions to ground-state properties in planar PA oligomers and focus on nonresonant Raman and IRAV intensities.

What is even more important, the empirical reference force field for pristine and isotopically labeled PA is directly based on accurate π-electronic shifts and vibrational frequencies in Ref. 2. As discussed in Sec. II, the different A in Eq. (6) and A^* in Eq. (9) then follow from a thorough analysis of pristine PA properties. Previous studies[29,30] adopt and revise parameters that reflect various compromises under the constraint $A=A^*$. Polymers with nondegenerate ground states are then accessible, at least approximately. By contrast, a reliable reference force field is a prequisite for our approach and has yet to be constructed for polymers with nondegenerate ground states. Their more complex backbone structure certainly makes the task more difficult and another parameter to describe the intrinsic gap is minimally needed. The limitation to PA oligomers imposed by the need for a reference makes possible quantitative vibrational analysis.

Our work primarily seeks to understand the physical origin of the peculiar vibrational properties of π-conjugated systems. The vibrational frequencies of PA segments are fully described by a single parameter, χ, that measures the π-electron susceptibility in response to the relevant coordinate[2,6] either the ECC in oligomers, or the DECC in soliton chains. This phenomenological picture is naturally understood in the approach proposed here. The χ values as extracted from experiment compare quantitatively with the model prediction.

We calculate nonresonant Raman intensities of ECC in oligomers and IRAV intensities of DECC in soliton chains. The superlinear increase of the IRAV intensity in soliton chains (see Fig. 5), associated with the nonlinear N dependence of the IRAV frequencies, leads to asymmetric IRAV bands even for simulated inhomogeneous PA samples with a symmetric distribution of chain lengths. Our simulations account well for the observed behavior of both ν_1 and ν_3 bands.[28] The calculated highly superlinear increase of the nonresonant Raman intensity of PA oligomers agrees with available experimental data on oligomers up to $\sim$40 sites.[23]

The N dependence of vibrational properties deserves further analysis. The geometrical distortion associated with the soliton defect extends over $\sim$14 sites. However, the physical properties of the soliton depend on the length of the chain where the soliton is embedded up to chain lengths well be-

yond 14 sites. The $\chi(N)$ curve in Fig. 5 (upper panel) does not saturates up to ~ 60 sites, suggesting that a soliton on an infinite chain explores ~ 60 sites: the geometrical length of the defect is ~ 14 sites, yet its coherence length, as suggested by χ, is about four times as large. Whereas this observation is far from trivial, it can be easily rationalized in terms of the well-known nonlocality of π electrons. More difficult is the different behavior of the infrared intensity that, as shown in Fig. 5, lower panel, is sensitive to the chain length up to over 100 sites, then suggesting an even larger coherence length. Even more impressive is the nonresonant Raman intensity of oligomers (Fig. 2, upper panel) that saturates at much longer chain-lengths than either the corresponding χ (Fig. 2, lower panel) or I_{IR}. In fact, the data in Fig. 2 suggest that true saturation occurs at $N>200$. We can understand the N dependence of I_{Ram} by noticing that the electronic polarizability [α in Eq. (14)] is largely dominated by the optical $1B_u$ excitation, so that it is roughly proportional to $1/\Delta$, Δ being the optical gap. The optical gap decreases with the chain length following a relation $\Delta \sim 4t\delta + B/N$, with B only slightly depending on δ.[31] Since the ECC coordinate modulates the alternation, we end up with $I_{\mathrm{Ram}} \sim 1/\Delta^4$. The proposed scaling of I_{Ram} with the optical gap is confirmed by the direct comparison with $1/\Delta^4$, as shown in Fig. 2, and easily explains the different N dependence of the different physical properties. In fact, the optical gap is expected to saturate when $B/N \to 0$, whereas I_{Ram} saturates when $4B/N \to 0$, and therefore at chain lengths about four times longer than the optical gap. As it has already been recognized for nonlinear optical (NLO) properties,[32,33] for a given coherence length of the electronic motion, as measured for instance by the length where Δ becomes independent of N, one will observe different saturation lengths for different quantities. In this respect the IR intensity of soliton chains apparently measures a nonlinearity of lower order than the Raman intensity, and, in fact, as shown in Fig. 5, lower panel, it approximately scales as $1/\Delta^2$.

The relation between vibrational intensities and NLO responses is not unexpected: IR absorption is the imaginary part of the linear polarizability ($\chi^{(1)}$) at vibrational frequencies, whereas the nonresonant Raman process is a contribution to the imaginary part of the second hyperpolarizability ($\chi^{(3)}$). In a different spirit, the IR intensity in soliton chains scales as the leading term in the perturbative expansion of the vibrational contribution to the static $\chi^{(1)}$, whereas the nonresonant Raman intensity of pristine PA gives the leading vibrational contribution to the static $\chi^{(3)}$.[34] IR and nonresonant Raman intensities are true ground-state properties whose calculation does not require excited-state properties such as transition energies or dipoles. The N dependence of vibrational intensities thus offers opportunities to follow the evolution of (low-frequency) nonlinear responses from conjugated molecules to polymers. The corresponding evolution of NLO coefficients is an active current research area.[1,35,36] The widths of NLO spectra and poorly characterized excited states hamper accurate N dependencies.

π-conjugated systems are intrinsically nonlinear, as demonstrated by the nonadditivity of their ground-state properties. π-electron fluctuations extending over large polymer portions are responsible for this nonlinearity. Understanding the physical behavior of these systems is difficult: the behavior of short segments does not imply any obvious information about longer chains and, at the same time, their responses to a given order need not give information about higher orders. Interpretative models that rationalize experimental data or detailed quantum-chemical calculations are therefore extremely useful. We have presented a simple yet reliable model, which accounts in a consistent framework for π-electron fluctuations and for the force field originated by the σ skeleton. This model is a good starting point to investigate the subtle interplay between electronic and nuclear degrees of freedom that governs the physics of conjugated polymers.

ACKNOWLEDGMENTS

The work at Parma was supported by the Italian Ministry of University and Scientific and Technological Research (MURST) under the project COFIN98, and by the National Research Council (CNR) within its ''Progetto Finalizzato Materiali Speciali per Tecnologie Avanzate II.'' The work in Princeton was supported by the National Science Foundation through Grant No. DMR-9530016.

[1] See, for instance, *Handbook of Conducting Polymers*, edited by T.A. Skotheim, R.L. Elsenbaumer, and J.R. Reynolds (Marcel Dekker, New York, 1998).
[2] Z.G. Soos, D. Mukhopadhyay, A. Painelli, and A. Girlando, in Ref. 1, p. 165.
[3] W.-P. Su, J.R. Schrieffer, and A.J. Heeger, Phys. Rev. Lett. **42**, 1698 (1979); Phys. Rev. B **22**, 2099 (1980).
[4] L. Salem, *The Molecular Orbital Theory of Conjugated Systems* (Benjamin, New York, 1966).
[5] A. Girlando, A. Painelli, and Z.G. Soos, Chem. Phys. Lett. **198**, 9 (1992).
[6] A. Girlando, A. Painelli, and Z.G. Soos, J. Chem. Phys. **98**, 7459 (1993).
[7] A. Girlando, A. Painelli, G.W. Hayden, Z.G. Soos, Chem. Phys. **184**, 139 (1994).
[8] Z.G. Soos, A. Girlando, and A. Painelli, Mol. Cryst. Liq. Cryst. Sci. Technol., Sect. A **256**, 711 (1994).
[9] H.C. Longuet-Higgins, L. Salem, Proc. R. Soc. London, Ser. A **251**, 172 (1959).
[10] C.A. Coulson, H.C. Longuet-Higgins, Proc. R. Soc. London, Ser. A **193**, 456 (1948).
[11] E.B. Wilson, J.C. Decius, and P. Cross, *Molecular Vibrations* (McGraw-Hill, New York, 1955).
[12] D. Vanderbilt and E.J. Mele, Phys. Rev. B **22**, 3939 (1980).
[13] S. Stafström and K.A. Chao, Phys. Rev. B **29**, 7010 (1983).
[14] B.S. Shastry, Phys. Rev. Lett. **50**, 633 (1983).
[15] F.L.J. Vos *et al.*, Phys. Rev. B **53**, 14 922 (1996).
[16] A.J. Heeger, S. Kivelson, J.R. Schrieffer, and W.-P. Su, Rev. Mod. Phys. **60**, 781 (1988).
[17] A. Painelli and A. Girlando, J. Chem. Phys. **84**, 5655 (1986).
[18] A. Girlando, A. Painelli, A. Girlando, L. Del Freo, and Z.G. Soos, Phys. Rev. B **56**, 15 100 (1997).

[19] M. Gussoni, C. Castiglioni, and G. Zerbi, in *Advances in Spectroscopy*, edited by R.J.H. Clarks and R.E. Hester (Wiley, New York, 1991), Vol. 19, p. 251.
[20] G. Orlandi, F. Zerbetto, and M.Z. Zgierski, Chem. Rev. **91**, 867 (1991).
[21] H.E. Schaffer, R.R. Chance, R.J. Silbey, K. Knoll, and R.R. Schrock, J. Chem. Phys. **94**, 4161 (1991).
[22] Z.G. Soos, G.W. Hayden, A. Girlando, and A. Painelli, J. Chem. Phys. **100**, 7144 (1994).
[23] M. Rumi, G. Zerbi, K. Müllen, G. Müllen, and M. Rebahn, J. Chem. Phys. **106**, 24 (1997).
[24] O. Lazareva and A.N. Shchegolikhn, Synth. Met. **84**, 991 (1997).
[25] H.O. Villar, M. Dupuis, and E. Clementi, Phys. Rev. B **37**, 2520 (1988).
[26] S. Suhai, Int. J. Quantum Chem. **42**, 193 (1992).
[27] B. Champagne, E. Deumens, and Y. Öhrn, J. Chem. Phys. **107**, 5433 (1997).
[28] E. Mulazzi, A. Ripamonti, C. Godon, S. Lefrant, and G. Leising, Synth. Met. **84**, 911 (1997); Phys. Rev. B **57**, 15 328 (1998).
[29] P.R. Surjan, H. Kuzmany, Phys. Rev. B **33**, 2615 (1986); J. Kürti and H. Kuzmany, *ibid.* **38**, 5634 (1988); **44**, 597 (1991).
[30] T. Danno, J. Kürti, and H. Kuzmany, Phys. Rev. B **43**, 4809 (1991).
[31] B.E. Kohler, C. Spangler, and C. Westerfield, J. Chem. Phys. **89**, 5422 (1988).
[32] F.C. Spano and Z.G. Soos, J. Chem. Phys. **99**, 9265 (1993).
[33] S. Tretiak, V. Chernyak, and S. Mukamel, Chem. Phys. Lett. **259**, 55 (1996).
[34] A. Painelli, Synth. Met. **101**, 218 (1999).
[35] I.D.W Samuel, I. Ledoux, C. Dhenaut, J. Zyss, H.H. Fox, R.R. Schrock, and R.J. Silbey, Science **265**, 1070 (1994).
[36] *Nonlinear Optical Materials: Theory and Modeling*, *ACS Symposium Series*, No. 628, edited by S.S. Karna and A.T. Yeates (ACS, Washington, D.C., 1996).